Weak measurement of qubit oscillations with strong response detectors: Violation of the fundamental bound imposed on linear detectors

HuJun Jiao,[1] Feng Li,[1] Shi-Kuan Wang,[2] and Xin-Qi Li[1,3,*]

[1]*State Key Laboratory for Superlattices and Microstructures, Institute of Semiconductors, Chinese Academy of Sciences, P.O. Box 912, Beijing 100083, China*

[2]*Department of Chemistry, Beijing Normal University, Beijing 100875, China*

[3]*Department of Physics, Beijing Normal University, Beijing 100875, China*

(Received 27 October 2008; revised manuscript received 18 January 2009; published 24 February 2009)

Qubit measurement by mesoscopic charge detectors has received great interest in the community of mesoscopic transport and solid-state quantum computation, and some controversial issues still remain unresolved. In this work, we revisit the continuous weak measurement of a solid-state qubit by single electron transistors (SETs) in nonlinear-response regime. For two SET models typically used in the literature, we find that the signal-to-noise ratio can violate the universal upper bound "4," which is imposed quantum mechanically on linear-response detectors. This different result can be understood by means of the cross correlation of the detector currents by viewing the two junctions of the single SET as two detectors. Possible limitation of the potential-scattering approach to this result is also discussed.

DOI: 10.1103/PhysRevB.79.075320 PACS number(s): 73.63.Kv, 03.65.Ta, 03.65.Yz, 73.23.−b

I. INTRODUCTION

The single electron transistor (SET) is a sensitive charge-state detector,[1–3] which promises the use for fast qubit readout in solid-state quantum computation. For *single-shot* measurement, i.e., in one run the qubit state is unambiguously determined, an important figure of merit is the detector's efficiency defined as the ratio of information-gained time and the measurement-induced dephasing time.[2] In the weakly responding regime, it was found that the SET has rather poor quantum efficiency.[2,4,5] However, a recent study showed that for strong response SET the quantum limit of an ideal detector can be reached, resulting in an almost pure-conditioned state.[6]

Rather than the single-shot measurement, a more implementable approach in experiment is the continuous weak measurement. This type of measurement allows the ensemble average of detector and qubit states, and the qubit coherent oscillation is read out from the spectral density of the detector. In continuous weak measurement, a remarkable result is the Korotkov-Averin (K-A) bound, originally with the following statement.[7] The interplay between the information acquisition and the backaction dephasing of the oscillations by the detector imposes a fundamental limit, equal to four, *on the signal-to-noise ratio (SNR) of the measurement.* The limit is universal, e.g., independent of the coupling strength between the detector and system, and results from the tendency of quantum measurement to localize the system in one of the measured eigenstates. In order to overcome the K-A bound, particular techniques, such as the quantum nondemolition (QND) measurement,[8] the quantum feedback control,[9] and the measurement with two detectors,[10] have been proposed. In this work, we investigate the continuous weak measurement by strongly responding SETs.[6,11] Remarkably, we find that for both models studied in Refs. 6 and 11, the SNR can violate the *universal* Korotkov-Averin bound. We can also provide an interpretation for this different result.

The paper is organized as follows. We begin in Sec. II with a model description for the measurement setup; then in Sec. III we turn to the method employed in this work. The numerical result of the spectral density of the measurement current is displayed in Sec. IV, and the interpretation for the K-A bound violation is carried out in Sec. V. Finally, the summary and concluding remarks are presented in Sec. VI.

II. MODEL

Consider a charge qubit—say—an electron in a pair of coupled quantum dots, measured by a single electron transistor, as schematically shown in Fig. 1. The entire system is described by the following Hamiltonian:

$$H = H_0 + H', \tag{1a}$$

$$H_0 = H_S + \sum_{\lambda=L,R} \epsilon_{\lambda k} d^\dagger_{\lambda k} d_{\lambda k}, \tag{1b}$$

$$H_S = \sum_{j=a,b} E_j |j\rangle\langle j| + \Omega(|a\rangle\langle b| + |b\rangle\langle a|) + E_c a_c^\dagger a_c + U n_a n_c, \tag{1c}$$

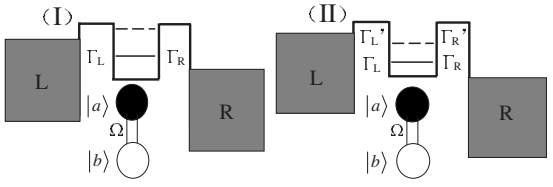

FIG. 1. Schematic model for a solid-state qubit measurement by SET. Model (I): the SET dot level is within the bias voltage for qubit state $|b\rangle$ but outside of it for state $|a\rangle$. Model (II): the SET dot level is between the Fermi levels for either $|b\rangle$ or $|a\rangle$ but with different coupling strengths to the leads, i.e., $\Gamma_{L/R}$ for $|b\rangle$ and $\Gamma'_{L/R}$ for $|a\rangle$.

$$H' = \sum_{\lambda=L,R;k} (\Omega_{\lambda k} a_c^\dagger d_{\lambda k} + \text{H.c.}) \equiv a_c^\dagger (f_{cL} + f_{cR}) + \text{H.c.} \tag{1d}$$

For simplicity, we assumed spinless electrons. The system Hamiltonian H_S contains a qubit and the SET central dot and their Coulomb interaction (the U term). For the qubit, we assumed that each dot has only one bound state, i.e., the logic states $|a\rangle$ and $|b\rangle$ with energies E_a and E_b, and with a coupling amplitude Ω. n_a is the number operator of qubit state $|a\rangle$, which equals to 1 for $|a\rangle$ occupied and 0 otherwise. For the SET, $a_c^\dagger$ (a_c) and $d_{\alpha k}^\dagger$ ($d_{\alpha k}$) are the electron creation (annihilation) operators of the central dot and reservoirs. $n_c \equiv a_c^\dagger a_c$ is introduced as the number operator of the SET dot. Similar to the previous work, we assumed that the SET works in the strong Coulomb-blockade regime, with only a single level E_c involved in the measurement process. Finally, H' describes the tunnel coupling of the SET dot to the leads, with amplitudes $\Omega_{\lambda k}$.

In this work, we consider two SET models as schematically shown in Fig. 1. In model (I), which was studied in Ref. 11, the SET dot level is within the bias voltage if the qubit is in state $|b\rangle$, but it locates above the Fermi levels when the qubit state is switched to $|a\rangle$. For state $|b\rangle$, a nonzero current I_b flows through the SET; however, for state $|a\rangle$, the SET current I_a is zero. Then, the qubit state can be discriminated from these different currents. In this model, the signal current $\Delta I \equiv |I_b - I_a|$ is twice the average current $\bar{I} \equiv (I_b + I_a)/2$. In this sense, it is not a weak response detector. In model (II), which allows to illustrate the crossover from weak to strong responses, the SET dot level is always between the Fermi levels of the two leads (for a qubit either in state $|b\rangle$ or in state $|a\rangle$) but with different coupling strengths to the leads, i.e., $\Gamma_{L(R)}$ and $\Gamma'_{L(R)}$. For the convenience of description, we further parametrize the tunnel couplings as $\Gamma_L(\Gamma'_L) = (1 \pm \xi)\bar{\Gamma}_L$, $\Gamma_R(\Gamma'_R) = (1 \pm \zeta)\bar{\Gamma}_R$, and $\gamma = \bar{\Gamma}_R/\bar{\Gamma}_L$. Here, $\bar{\Gamma}_{L(R)} = (\Gamma_{L(R)} + \Gamma'_{L(R)})/2$ denote the average couplings, while ξ and ζ characterize the response strength of the detector to the qubit. In this context, we would like to stress that most previous works were largely restricted in the weak response regime by assuming $\xi \ll 1$ and $\zeta \ll 1$, except in Ref. 6 where the quantum efficiency was investigated in the strong response regime using this model.

III. FORMALISM

In continuous weak measurement, the detector's output is characterized by the current and noise spectral density. For their calculation, the most efficient approach is the particle-number-resolved master equation.[2] In obtaining it, the qubit and SET dot are regarded as the system of interest, while the two leads of the SET as an environment; the tunnel coupling H' of the SET is treated perturbatively as an interaction between them. Up to the dominant second order of H', following Ref. 12, we have

$$\dot{\rho}^{(n_R)} = -i\mathcal{L}\rho^{(n_R)} - \frac{1}{2}\{[a_c^\dagger, A_{cL}^{(-)}\rho^{(n_R)} - \rho^{(n_R)}A_{cL}^{(+)}] + a_c^\dagger A_{cR}^{(-)}\rho^{(n_R)} + \rho^{(n_R)}A_{cR}^{(+)}a_c^\dagger - [a_c^\dagger \rho^{(n_R+1)}A_{cR}^{(+)} + A_{cR}^{(-)}\rho^{(n_R-1)}a_c^\dagger] + \text{H.c.}\}. \tag{2}$$

$\rho^{(n_R)}$ is the reduced density operator of the *system* conditioned on the electron number "n_R" tunneled through the right junction (a similar equation holds also for the left junction). For simplicity, throughout this paper we use the convention $\hbar = e = k_B = 1$. In Eq. (2) the Liouvillian $\mathcal{L}$ is defined by $\mathcal{L}(\cdots) = [H_S, \cdots]$, and the operators $A_{c\lambda}^{(\pm)} \equiv C_\lambda^{(\pm)}(\pm\mathcal{L})a_c$. The superoperators $C_\lambda^{(\pm)}(\pm\mathcal{L})$ are the generalized spectral functions $C_\lambda^{(\pm)}(\pm\mathcal{L}) = \int_{-\infty}^{+\infty} dt C_\lambda^{(\pm)}(t) e^{\pm i\mathcal{L}t}$, where the bath correlation functions $C_\lambda^{(+)}(t) = \langle f_{c\lambda}^\dagger(t) f_{c\lambda}\rangle_B$ and $C_\lambda^{(-)}(t) = \langle f_{c\lambda}(t) f_{c\lambda}^\dagger\rangle_B$, and the average $\langle\cdots\rangle_B \equiv \text{Tr}_B[(\cdots)\rho_B]$, with ρ_B local thermal equilibrium state of the SET leads determined by the respective chemical potentials.

Rich information is contained in the above particle-number-resolved master equation, since the conditional density matrix $\rho^{(n_R)}(t)$ is directly related to the distribution function $P(n_R, t) = \text{Tr}[\rho^{(n_R)}(t)]$, where the trace is over the system states. For instance, by virtue of this relation, the measurement current can be obtained as[12]

$$I_R(t) = \sum_{n_R} \text{Tr}\{n_R \dot{\rho}^{(n_R)}(t)\} = \text{Re Tr}[(a_c^\dagger A_{cR}^{(-)} - A_{cR}^{(+)} a_c^\dagger)\rho(t)], \tag{3}$$

where $\rho(t) \equiv \Sigma_{n_R} \rho^{(n_R)}(t)$ satisfies the usual *unconditional* master equation, by summing the above Eq. (2) over n_R.

In continuous weak measurement, the detector's power spectral density contains very useful information of the qubit's coherent oscillation. Formally, the noise spectrum of the current consists of three terms:[13] $S(\omega) = \alpha S_L(\omega) + \beta S_R(\omega) - \alpha\beta\omega^2 S_N(\omega)$, with $S_{L/R}(\omega)$ the noise of the left (right) junction current $I_{L/R}(t)$ and $S_N(\omega)$ the fluctuations of the electron number $N(t)$ on the central dot of the SET. α and β are two coefficients determined by the junction capacitances[13] and satisfy $\alpha + \beta = 1$. Further, for $S_{L/R}(\omega)$, it follows the MacDonald's formula:

$$S_\lambda(\omega) = 2\omega \int_0^\infty dt \sin \omega t \frac{d}{dt}[\langle n_\lambda^2(t)\rangle - (\bar{I}t)^2], \tag{4}$$

where $\bar{I}$ is the stationary current and $\langle n_\lambda^2(t)\rangle = \Sigma_{n_\lambda} n_\lambda^2 \text{ Tr } \rho^{(n_\lambda)}(t) = \Sigma_{n_\lambda} n_\lambda^2 P(n_\lambda, t)$. In practice, instead of directly solving $P(n_\lambda, t)$, the reduced quantity $\langle n_\lambda^2(t)\rangle$ can be obtained more easily by constructing its equation of motion[12] based on the particle-number-resolved master equation Eq. (2). In this way, we obtain

$$\frac{d}{dt}\langle n_\lambda^2(t)\rangle = \text{Tr}[2\mathcal{J}_\lambda^{(-)} Q_\lambda(t) + \mathcal{J}_\lambda^{(+)}\rho^{\text{st}}]. \tag{5}$$

Here the particle-number matrix is defined as $Q_\lambda(t) \equiv \Sigma_{n_\lambda} n_\lambda \rho^{(n_\lambda)}(t)$ and ρ^{st} denotes the stationary state. The superoperators $\mathcal{J}_\lambda^{(\pm)}$ are defined by

$$\mathcal{J}_\lambda^{(\pm)}(\cdots) = \frac{1}{2}[A_{c\lambda}^{(-)}(\cdots)a_c^\dagger \pm a_c^\dagger(\cdots)A_{c\lambda}^{(+)} + a_c(\cdots)A_{c\lambda}^{(-)\dagger} \pm A_{c\lambda}^{(+)\dagger}(\cdots)a_c]. \tag{6}$$

Inserting Eq. (5) into Eq. (4), in the frequency domain we obtain

$$S_\lambda(\omega) = 4\omega\ \mathrm{Im}\{\mathrm{Tr}[\mathcal{J}_\lambda^{(-)}\tilde{Q}_\lambda(\omega)]\} + 2\ \mathrm{Tr}\ \mathcal{J}_\lambda^{(+)}\rho^{\mathrm{st}} - 8\pi\bar{I}^2\delta(\omega), \tag{7}$$

where $\tilde{Q}_\lambda(\omega)=\int_0^\infty Q_\lambda(t)e^{i\omega t}$. For $\tilde{Q}_\lambda(\omega)$, we can obtain it by solving a set of algebraic equations after Laplace transforming the equation of motion of $Q_\lambda(t)$, as clearly described in Ref. 13.

For $S_N(\omega)$, which is the Fourier transform of the correlation function $\langle\{N(t),N(0)\}\rangle$, following Ref. 13, the quantum regression theorem gives

$$S_N(\omega) = 2\ \mathrm{Re}\ \mathrm{Tr}\{N[\tilde{\sigma}(\omega) + \tilde{\sigma}(-\omega)]\}. \tag{8}$$

$\tilde{\sigma}(\omega)$ is introduced as the Laplace transform of $\sigma(t) \equiv \mathrm{Tr}_B[U(t)N\rho^{\mathrm{st}}\rho_B U^\dagger(t)]$, where $U(t)=e^{-iH_S t}$. Obviously, $\sigma(t)$ satisfies the same equation of the reduced density matrix $\rho(t)$. The only difference is the initial condition for $\sigma(t)$, which is $\sigma(0)=N\rho^{\mathrm{st}}$.

IV. RESULTS

For both models in Fig. 1, the states involved are $|1\rangle \equiv |0a\rangle$, $|2\rangle \equiv |0b\rangle$, $|3\rangle \equiv |1a\rangle$, and $|4\rangle \equiv |1b\rangle$. In this notation $|0(1)a(b)\rangle$ means that the SET dot is empty (occupied) and the qubit is in state $|a(b)\rangle$. Applying Eq. (2) to model (I) results in

$$\dot{\rho}_{11}^{(n_R)} = i\Omega[\rho_{12}^{(n_R)} - \rho_{21}^{(n_R)}] + \Gamma_L\rho_{33}^{(n_R)} + \Gamma_R\rho_{33}^{(n_R-1)}, \tag{9a}$$

$$\dot{\rho}_{22}^{(n_R)} = i\Omega[\rho_{21}^{(n_R)} - \rho_{12}^{(n_R)}] - \Gamma_L\rho_{22}^{(n_R)} + \Gamma_R\rho_{44}^{(n_R-1)}, \tag{9b}$$

$$\dot{\rho}_{12}^{(n_R)} = -i\epsilon\rho_{12}^{(n_R)} + i\Omega[\rho_{11}^{(n_R)} - \rho_{22}^{(n_R)}] - \frac{\Gamma_L}{2}\rho_{12}^{(n_R)} + \frac{\Gamma_L}{2}\rho_{34}^{(n_R)} + \Gamma_R\rho_{34}^{(n_R-1)}, \tag{9c}$$

$$\dot{\rho}_{33}^{(n_R)} = i\Omega[\rho_{34}^{(n_R)} - \rho_{43}^{(n_R)}] - (\Gamma_R+\Gamma_L)\rho_{33}^{(n_R)}, \tag{9d}$$

$$\dot{\rho}_{44}^{(n_R)} = i\Omega[\rho_{43}^{(n_R)} - \rho_{34}^{(n_R)}] + \Gamma_L\rho_{22}^{(n_R)} - \Gamma_R\rho_{44}^{(n_R)}, \tag{9e}$$

$$\dot{\rho}_{34}^{(n_R)} = -i(\epsilon+U)\rho_{34}^{(n_R)} + i\Omega[\rho_{33}^{(n_R)} - \rho_{44}^{(n_R)}] + \frac{\Gamma_L}{2}\rho_{12}^{(n_R)} - \left(\Gamma_R + \frac{\Gamma_L}{2}\right)\rho_{34}^{(n_R)}. \tag{9f}$$

Here, $\epsilon=E_a-E_b$ and $\Gamma_{L/R}=2\pi|\Omega_{L/R}|^2 g_{L/R}$, with $g_{L/R}$ the density of states of the SET leads. For simplicity, the assumption of wide-band limit implies $\Omega_{L/R}\equiv\Omega_{L/Rk}$ and makes $\Gamma_{L/R}$ energy independent. Also, low temperature and $U\gg\Omega$ were assumed to further simplify the equations. Similarly, for model (II), we have

$$\dot{\rho}_{11}^{(n_R)} = i\Omega[\rho_{12}^{(n_R)} - \rho_{21}^{(n_R)}] - \Gamma_L'\rho_{11}^{(n_R)} + \Gamma_R'\rho_{33}^{(n_R-1)}, \tag{10a}$$

$$\dot{\rho}_{22}^{(n_R)} = i\Omega[\rho_{21}^{(n_R)} - \rho_{12}^{(n_R)}] - \Gamma_L\rho_{22}^{(n_R)} + \Gamma_R\rho_{44}^{(n_R-1)}, \tag{10b}$$

$$\dot{\rho}_{12}^{(n_R)} = -i\epsilon\rho_{12}^{(n_R)} + i\Omega[\rho_{11}^{(n_R)} - \rho_{22}^{(n_R)}] - \frac{\Gamma_L+\Gamma_L'}{2}\rho_{12}^{(n_R)} + \frac{\Gamma_R+\Gamma_R'}{2}\rho_{34}^{(n_R-1)}, \tag{10c}$$

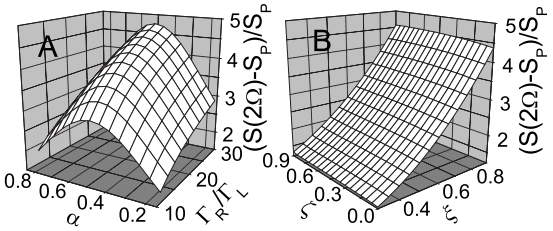

FIG. 2. Signal-to-noise ratio: (A) for model (I) and (B) for model (II). For model (I), we take $\Gamma_L\equiv\Gamma$ as the energy unit and assume that $\mu_{L(R)}=\pm 50\Gamma$, $\Omega=2\Gamma$, and $U=80\Gamma$. For model (II), we use $\bar{\Gamma}_L\equiv\bar{\Gamma}$ as the energy unit and assume that $\Omega=\bar{\Gamma}$, $U=50\bar{\Gamma}$, $\bar{\Gamma}_R=30\bar{\Gamma}$, and $\alpha=\beta=1/2$. Also, zero temperature and $E_a=E_b$ are assumed.

$$\dot{\rho}_{33}^{(n_R)} = i\Omega[\rho_{34}^{(n_R)} - \rho_{43}^{(n_R)}] + \Gamma_L'\rho_{11}^{(n_R)} - \Gamma_R'\rho_{33}^{(n_R)}, \tag{10d}$$

$$\dot{\rho}_{44}^{(n_R)} = i\Omega[\rho_{43}^{(n_R)} - \rho_{34}^{(n_R)}] + \Gamma_L\rho_{22}^{(n_R)} - \Gamma_R\rho_{44}^{(n_R)}, \tag{10e}$$

$$\dot{\rho}_{34}^{(n_R)} = -i(\epsilon+U)\rho_{34}^{(n_R)} + i\Omega[\rho_{33}^{(n_R)} - \rho_{44}^{(n_R)}] + \frac{\Gamma_L+\Gamma_L'}{2}\rho_{12}^{(n_R)} - \frac{\Gamma_R+\Gamma_R'}{2}\rho_{34}^{(n_R)}. \tag{10f}$$

Except for the conditions leading to model (II), other parameters are the same as above.

In continuous weak measurement of qubit oscillation, the signal is manifested as a peak in the noise spectrum at the qubit oscillation frequency 2Ω, while the measurement effectiveness is characterized by the SNR, i.e., the *peak-to-pedestal* ratio. We denote the noise pedestal by S_p and obtain it conventionally from $S(\omega\to\infty)$. In Fig. 2 we show the dependence of the SNR on the detector's configuration symmetries.

The result of model (I) is shown in Fig. 2(A), where we see that both the tunnel- and capacitive-coupling symmetries crucially affect the measurement effectiveness. For the effect of tunnel-coupling asymmetry Γ_R/Γ_L, the basic reason is that, with the increase of Γ_R/Γ_L, the interaction time of the detector electron with the qubit is decreased. Thus the detector's backaction is reduced and the SNR is enhanced.[11] For the effect of capacitive coupling, its degree of asymmetry affects the contribution weight of the cross correlation between $I_L(t)$ and $I_R(t)$ to the entire circuit noise. Specifically, the cross correlation has a more important contribution for more symmetric coupling, as shown in Fig. 2(A) by the α dependence. This is because, as we shall demonstrate below, the cross correlation has much higher *peak-to-pedestal* ratio than the autocorrelation.

An unexpected feature observed in Fig. 2(A) is that under proper conditions, say, the symmetric capacitive coupling and strongly asymmetric tunnel coupling, the SNR can exceed "4," which is the upper bound quantum mechanically limited on *any linear-response detectors*.[7] However, to our knowledge, whether this upper bound is applicable to a *nonlinear*-response detector is so far unclear *in priori*, since in this case the linear-response relation between the current

and qubit state breaks down then the subsequent Cauchy-Schwartz-inequality based argument leading to the upper bound "4" does not work.[10]

To support the above reasoning, we further check model (II). The result is presented in Fig. 2(B). As explained in the model description, the parameters ξ and ζ used here characterize, respectively, the left and right tunnel-coupling responses to the qubit states. Shown in Fig. 2(B) is for an asymmetric tunnel-coupling detector, with $\gamma \equiv \bar{\Gamma}_R/\bar{\Gamma}_L = 30$, which can lead to higher SNR, because of the weaker back-action from the detector, similar to model (I). Here we find that the SNR is insensitive to the right junction response, ζ but sensitive to the left one, ξ. Again, in this model, we observe that the SNR can violate the K-A bound "4" in the strong response regime.

V. UNDERSTANDING THE VIOLATION OF THE K-A BOUND

Since $I(t)=\alpha I_L(t)+\beta I_R(t)$, the current correlator $\langle I(t)I(0)\rangle$ contains the component $S_{LR}(t) \equiv \langle I_L(t)I_R(0)+I_R(t)I_L(0)\rangle$, i.e., the cross correlation. In the previous results, we already observed that for more symmetric capacitive coupling the SNR is larger and reaches the maximum at $\alpha=\beta=1/2$. This feature indicates that the cross correlation has an effect of enhancing the SNR.

Indeed, for the SET detector, both the left and right junction currents (I_L and I_R) contain the information of qubit state, so their "signal" parts are correlated. This leads us to viewing heuristically the two junctions of a single SET as two detectors, such as the scheme of qubit measurement by two quantum point contacts (QPC) proposed recently by Jordan and Büttiker,[10] where they found that the SNR of the cross correlation can strongly violate the K-A bound because of the negligibly small pedestal of the cross noise. In our case, since $I_L(t)$ and $I_R(t)$ are subject to a constraint from charge conservation, the cross noise background of $I_L(t)$ and $I_R(t)$ does not vanish in principle, unlike the two independent QPC detectors.[10] Nevertheless, the pedestal of the cross noise of the SET is much smaller than that of the autocorrelation, which leads to an enhanced SNR in the spectral density of the total circuit current, and to the violation of the K-A bound.

In Fig. 3 we plot the signal-to-noise ratio versus the tunnel-coupling asymmetry Γ_R/Γ_L for model (I) and $\bar{\Gamma}_R/\bar{\Gamma}_L$ for model (II). To more clearly show the effect of the cross correlation, in Fig. 3(A) we display the results in the presence of cross correlation (the solid and dashed lines) and after removing it (the dotted and dot-dashed lines). We see that the former can violate the K-A bound, while the latter cannot. In Fig. 3(B) we separately plot the SNR of the cross correlation scaled by the noise pedestal S_p of the entire circuit current. This illustrates the role of the cross noise in enhancing the SNR and violating the K-A bound.

In Fig. 4 the spectral density of the cross correlation scaled by its own noise pedestal is shown representatively. As mentioned above, since at the high-frequency limit the cross noise pedestal is negligibly small, here we artificially (but more physically in some sense) define the pedestal at a

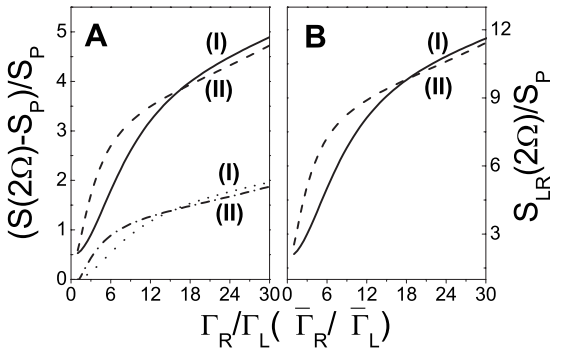

FIG. 3. Signal-to-noise ratio versus tunnel-coupling asymmetry; Γ_R/Γ_L for model (I) and $\bar{\Gamma}_R/\bar{\Gamma}_L$ for model (II). In (A) the solid and dashed lines are the result in the presence of cross correlation, while the dotted and dot-dashed lines are the result after removing it. In (B) the mere cross correlation is plotted. S_p is the pedestal noise of the entire circuit current. $\xi=\zeta=0.9$; other parameters are the same as in Fig. 2.

finite frequency, e.g., twice the qubit oscillation frequency. Obviously, the giant SNR of the cross correlation has drastically violated the K-A bound. This result indicates that in qubit measurement by the SET, one can exploit the cross correlation rather than the auto one as usual to probe the coherent oscillations. In practice, such a scheme is simpler than the technique of QND measurement[8] and holds the most advantages of the SET over QPC. In recent years, the cross correlation in mesoscopic transport is an extensive research subject. Its measurement in experiment is also possible, for instance, using the nearby-QPC counting technique.[14]

VI. CONCLUDING REMARKS

In summary, we have investigated the continuous weak measurement of qubit oscillations by a nonlinear-response SET and demonstrated that the signal-to-noise ratio can violate the universal Korotkov-Averin bound. The violation has been understood by the role of the cross correlation of the detector's currents. This interpretation also leads to the useful implication to the experiment.

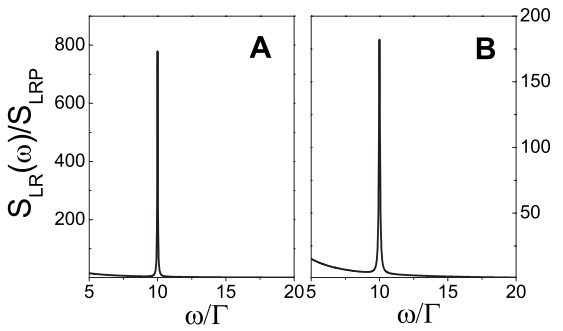

FIG. 4. Spectral density of the cross correlation scaled by its own pedestal, here which is defined at twice the Rabi frequency of the qubit oscillations. Parameters for model (I) in (A): $\Gamma_L=0.05\Gamma$, $\Gamma_R=0.5\Gamma$, and $\Omega=5\Gamma$. Parameters for model (II) in (B): $\bar{\Gamma}_L=0.05\Gamma$, $\bar{\Gamma}_R=0.5\Gamma$, $\Omega=5\Gamma$, and $\xi=\zeta=0.9$. Γ in this figure is used as an energy unit; other conventions are the same as in Fig. 2.

Finally, additional remarks may be relevant to the present study. In the past decade, qubit measurement by mesoscopic charge detectors (typically QPC and SET) has received great interest in the community of mesoscopic transport and solid-state quantum computation. Owing to the many fundamental problems underlying, this interesting field is still alive, with many issues unresolved. For single-shot measurement, attention was focused on the quantum efficiency. In this context, theories based on concepts such as information acquisition and loss, and detector's backaction, were developed. However, such study was largely relevant to the QPC detector, which can be well described by a formal potential-scattering theory.[15–17] For SET detector, the scattering matrix description is not well suited. In fact, the quantum efficiency of the SET remains a controversial issue.[6]

For continuous weak measurement of qubit oscillations based also on the formal potential-scattering approach, the obtained K-A bound is important for its universal nature, i.e., valid for arbitrary linear detectors. For the SET, previous studies for qubit measurement were largely restricted to linear-response regime.[2] In Ref. 11, the SET (model (I) in our work) is in fact a strongly responding detector. However, the SNR was found there to be lower than three, thus leading to a conclusion that it cannot reach the ideal value "4" of QPC. In Ref. 10, the key conclusion was that by using two QPCs the SNR of the cross correlation can drastically violate the K-A bound. Therefore, the violation of the K-A bound for *a single detector* is not at all apparent *in priori*. Moreover, it is unclear to us how to apply the potential-scattering theory to SET detector and how to employ the cross correlation in that language to interpret the enhancement of SNR. Using the scattering approach, the nonlinear-response quantum measurement seems difficult to be handled. We anticipate that the present work can inspire further efforts on more general nonlinear-response detectors. To relate the SNR to quantum efficiency from the information aspect is also of great interest. In Ref. 10, the conditions of reaching the K-A bound and reaching the quantum-limited measurement coincide. However, in our recent work on the double-dot SET,[18] we found that they are different. Work along this line is in progress and will be presented in the forthcoming publication.

ACKNOWLEDGMENTS

This work was supported by the National Natural Science Foundation of China under Grants No. 60425412 and No. 90503013 and the Major State Basic Research Project under Grant No. 2006CB921201.

*xqli@red.semi.ac.cn

[1] M. H. Devoret and R. J. Schoelkopf, Nature (London) **406**, 1039 (2000).
[2] Yu. Makhlin, G. Schön, and A. Shnirman, Rev. Mod. Phys. **73**, 357 (2001).
[3] W. Lu, Z. Ji, L. Pfeifer, K. W. West, and A. J. Rimberg, Nature (London) **423**, 422 (2003).
[4] A. N. Korotkov, Phys. Rev. B **63**, 085312 (2001); **63**, 115403 (2001).
[5] D. Mozyrsky, I. Martin, and M. B. Hastings, Phys. Rev. Lett. **92**, 018303 (2004).
[6] N. P. Oxtoby, H. M. Wiseman, and H. B. Sun, Phys. Rev. B **74**, 045328 (2006).
[7] A. N. Korotkov and D. V. Averin, Phys. Rev. B **64**, 165310 (2001).
[8] D. V. Averin, Phys. Rev. Lett. **88**, 207901 (2002); A. N. Jordan and M. Büttiker, Phys. Rev. B **71**, 125333 (2005).
[9] S. K. Wang, J. S. Jin, and X. Q. Li, Phys. Rev. B **75**, 155304 (2007).
[10] A. N. Jordan and M. Büttiker, Phys. Rev. Lett. **95**, 220401 (2005).
[11] S. A. Gurvitz and G. P. Berman, Phys. Rev. B **72**, 073303 (2005).
[12] X. Q. Li, P. Cui, and Y. J. Yan, Phys. Rev. Lett. **94**, 066803 (2005).
[13] J. Y. Luo, X. Q. Li, and Y. J. Yan, Phys. Rev. B **76**, 085325 (2007).
[14] S. Gustavsson, R. Leturcq, B. Simovic, R. Schleser, T. Ihn, P. Studerus, K. Ensslin, D. C. Driscoll, and A. C. Gossard, Phys. Rev. Lett. **96**, 076605 (2006); T. Fujisawa, T. Hayashi, R. Tomita, and Y. Hirayama, Science **312**, 1634 (2006).
[15] S. Pilgram and M. Buttiker, Phys. Rev. Lett. **89**, 200401 (2002).
[16] A. A. Clerk, S. M. Girvin, and A. D. Stone, Phys. Rev. B **67**, 165324 (2003).
[17] D. V. Averin and E. V. Sukhorukov, Phys. Rev. Lett. **95**, 126803 (2005).
[18] H. J. Jiao, X. Q. Li, and J. Y. Luo, Phys. Rev. B **75**, 155333 (2007).